CR-73070

0501

GPO PRICE $ _____

CFSTI PRICE(S) $ _____

Hard copy (HC) 3.00

Microfiche (MF) .50

ff 653 July 65

FACILITY FORM 602

N67 11985
(ACCESSION NUMBER)

42
(PAGES)

CR-73070
(NASA CR OR TMX OR AD NUMBER)

1
(CODE)

04
(CATEGORY)

SUMMARY TECHNICAL REPORT
CONTRACT NO. NAS 2-2366

RESEARCH AND DEVELOPMENT PROGRAM FOR RADIATION MEASUREMENTS OF RADIOBIOLOGICAL HAZARDS OF MAN IN SPACE

1 AUGUST 1965 through 31 JULY 1966

HUGHES RESEARCH LABORATORIES
Malibu, California

a division of hughes aircraft company

RESEARCH AND DEVELOPMENT PROGRAM FOR RADIATION MEASUREMENTS OF RADIOBIOLOGICAL HAZARDS OF MAN IN SPACE

Summary Technical Report
NAS 2-2366

1 August 1965 through 31 July 1966

TABLE OF CONTENTS

LIST OF ILLUSTRATIONS

FOREWORD

The research carried out under contract number NAS 2-2366 with the NASA Ames Laboratory has been accomplished in cooperation with the department of Radiology of the University of California at Los Angeles. The program has been under the direction of Dr. Norman A. Baily, Manager, Space Sciences Department of the Hughes Research Laboratories and Professor of Radiology in Residence at the University of California at Los Angeles. The personnel assigned or contributing to this program are Mr. Jerald W. Hilbert, Mr. Frederick W. Cleary, and Dr. R. Ted Nichols of the Space Sciences Department of the Hughes Research Laboratories; Mr. Raymond L. Tanner and Professor Amos Norman, both of the Department of Radiology of the University of California at Los Angeles.

Availability of the cyclotron beams has been made possible through the cooperation of Professor J. Reginald Richardson of the Department of Physics, University of California at Los Angeles; Dr. C. A. Tobias of the Donner Laboratory, University of California at Berkeley; and Mr. Andrew Koehler of Harvard University.

We should also like to acknowledge the financial support given to Mr. Tanner by a U.S.P.H.S. training grant and by the NASA through a sub-grant from the UCLA Space Sciences Center which was grant #NASA-237-62.

I. INTRODUCTION

This research program was undertaken to develop and apply methods for measuring radiobiologically significant dosimetric quantities to be used for the evaluation of radiation hazards associated with manned space flights and for the evaluation of high energy proton irradiations of cells and whole animals. The effects of radiation depend not only upon absorbed dose and its distribution within the biological entity under study, but also upon the manner in which energy is deposited on a microscopic scale within the absorbing material. This is evident from the fact that radiations of different linear energy transfer (LET) will produce different biological effects even when the absorbed dose and dose rate are identical. Many studies have attempted to relate relative biological effectiveness (RBE) to the LET distribution of the dose within the biological entity being observed. The pioneering work in this area was done by Rossi and co-workers[1, 2] using spherical energy sensors for the determination of LET spectra. However, inherent limitations of the LET concept have been brought out through their work and they have proposed several alternative parameters[3-5] designed to facilitate a study of energy deposition distributions in truly microscopic volumes. Further studies by us have shown that for charged particles, additional modifications of these concepts are necessary.

The absorbed dose at a point is defined only when the absorbed energy divided by the mass reaches a constant ratio for successively smaller volume elements containing the point. However, this constant value must obtain for volume elements still large enough to contain a great many individual particle interactions, otherwise significant statistical fluctuations in this quantity will appear. Since energy is imparted to the medium by discrete interaction events in or near charged particle tracks it is evident that the absorbed energy density may have large variations on a microscopic scale even when the absorbed dose is quite uniform over macroscopic volumes. A knowledge of these local energy density variations is essential for fundamental studies of many radiation effects.

This research program represents an effort to define both the macroscopic and microscopic distribution of dose deposited by high energy protons in tissue with a view toward expanding the basic ideas inherent in Rossi's concepts and, if possible, developing improved concepts and methods while studying fundamental parameters. It is apparent that one meaningful way of expressing these concepts must certainly be the energy deposited per event in a biologically meaningful volume of proper size and shape.

Studies of the center line depth dose distributions for high energy protons were designed to elucidate the distribution of absorbed dose on a macroscopic scale. These studies have been greatly extended during the past year to include center line depth dose distributions for protons with energies of 20, 45, 137, 220, 260, 630, and 730 MeV. The distributions for the 630 and 730 MeV protons show a very rapid initial rise in dose with tissue depth which had not previously been predicted on theoretical grounds for these energies. The distributions for 20, 45, and 137 MeV protons are characterized by a gradual increase of dose with tissue depth, followed by a sharp peak as the protons approach the end of their range. The intermediate energy curves should actually not be taken to be center line depth dose distributions for beams of pure 220 MeV and 260 MeV protons, since both of these beams were obtained by drastic degradation of the 730 MeV proton beam and are thought to be rather severely contaminated with neutrons and/or gamma rays.

The second aspect of the work has been concerned with developing and applying methods for measuring microscopic dose distributions. Such distributions consist of energy deposited per event in biologically meaningful volumes. The aim in this phase of the study is to perfect several different types of tissue-equivalent proportional counters which may be used to simulate a wide range of biologically meaningful tissue volumes, and to determine the microscopic dose distributions produced by various radiations in these simulated volumes. These distributions will then be used to analyze the distributions obtained in very small, spherical, solid state detectors. In order to obtain meaningful microscopic dose distributions, of course, the collection efficiency and gas multiplication must be uniform at all operating voltages and gas pressures for pulses formed by particles passing through any portion of the chamber volume. These and related properties of several electrode configurations have been carefully examined using a brass chamber simulating the electrode and collecting volume of the tissue-equivalent chambers, as well as with the tissue-equivalent chambers themselves using high energy proton beams. A study of the resolution (FWHM) of the initial electrode in the brass test chamber, as a function of operating voltage and gas pressure, turned up some rather disturbing results. It was found that as the pressure was increased above 2.00 cm Hg the resolution of the peak due to a collimated α-source continuously deteriorated. Further, at each pressure investigated the resolution deteriorated with an increase in voltage. Similar indications of serious collection problems at extremes of pressure and voltage were observed by examining the response to an uncollimated α-source located on the wall of the chamber. Interestingly enough, it was discovered that this test of performance is not sufficient to insure that good collection efficiency through the whole chamber volume has been attained.

As detailed previously, the explorations of uniformity of volume response using the proton beams have been done by using a small frontal area silicon, lithium-drifted, p-i-n detector in coincidence with the chamber to select a portion of the proportional counter sensitive volume for examination. It was mentioned in the previous summary technical report that an effect then thought to be due to an interaction between the protons and the walls of the tissue-equivalent chamber had prevented the accumulation of coincidence spectra in the new experimental area. This phenomena was carefully examined and has been determined to be a natural feature of the proton scattering pattern from the polyethylene target generally used in the primary experiment at the cyclotron. It has therefore been possible to obtain additional useful data using the coincidence method. Further tests using the coincidence method in conjunction with a variable delay gate generator, to compensate for the transit time of the initial electrons to the center electrode, has indicated that the initial electrode design does not collect pulses formed in the outer part of the sensitive volume. The fact that it was the electrode design which is deficient was confirmed by a series of experiments in which the spherical tissue-equivalent chamber was used as an ionization chamber, and its saturation characteristics studied under a number of conditions using several electrode designs. In addition, substitution of methane for the normal He-CO_2 mixture in the brass chamber resulted in essentially the same anomalous behavior at extremes of pressure and voltage discussed above, indicating that it was not the gas which was at fault. An investigation of several possible new electrode designs has been carried out. Improved chamber performance has been obtained using a 0.003" stainless steel wire stretched completely across the spherical cavity. The new end plugs designed for this electrode also permit the tissue-equivalent chamber to be used as a flow system, which eliminates any possibility of gas contamination which might contribute to poor collection properties. This also insures constant gas multiplication and facilitates changes in gas pressure. In view of the fact that the initial electrode design turned out to have poor collection properties even though its uniformity of volume response had appeared quite acceptable using the angled alpha source as a probe, it became obvious that a much better test was needed to evaluate any new electrode designs. The brass test chamber has thus been altered to permit a much more thorough examination of the uniformity of volume response using a collimated α-source or monoenergetic electrons from the β-ray spectrometer. The new design permits a collimated beam to be directed along seven different parallel paths, consisting of a path through the center and three pairs of paths at 1 cm and 2 cm from the center, each subsequent pair being rotated 45^{o}, thus completely mapping one quadrant of the spherical volume.

The new electrode design incorporates a guard ring. This serves two purposes. First, it allows the chamber to be used as an ionization chamber. Second, field distortions can be corrected by proper choice of the guard ring operating potential.

II. CENTER LINE DEPTH DOSE STUDIES - HIGH ENERGY PROTONS

A. Experimental Measurements

Studies of the center line depth dose distributions delivered to tissue by protons having energies extending up to 730 MeV are designed to elucidate the distribution of absorbed dose on a macroscopic scale. These studies have been greatly extended during the past year to include center line depth dose distributions for protons with energies of 20, 45, 137, 220, 260, 630, and 730 MeV. The extrapolation chamber technique and experimental procedure utilized for these measurements were discussed in detail in the last summary technical report. In brief, the measurements consist of the absorbed dose as a function of depth in a polystyrene phantom. The absorbed dose is measured with an extrapolation chamber using a modified Townsend Balance circuit or through integration of the charge collected during the time required to collect a standard charge collected by a transmission monitor chamber.

The center line depth dose curves for 730 MeV and 630 MeV protons were included in the last summary technical report, but additional data has been obtained since that time. First, it should be mentioned that due to the use of an erroneous value for the density of the carbon beam degrader used the curve previously labelled as due to 600 MeV protons is actually that for 630 MeV protons. Secondly, additional data has been taken to finalize the exact shape of the sharp initial rise in the center line depth dose curve for 730 MeV protons. The completed data for 730 MeV protons is shown in curve A of Figs. 1 and 2. This new data very definitely reconfirms the validity of the previous measurements as well as providing more detail to this very important initial and sharply rising portion of the curve.

The center line depth dose distributions for protons with energies of 20 MeV and 45 MeV are shown in Figs. 3 and 4, respectively. Both of these energies were obtained directly (undegraded) from the UCLA 50 MeV Alternating Gradient Cyclotron by adjustment of machine parameters. As neither of these beams had previously been used in the spread-out mode necessary for meaningful center line depth dose measurements, it was necessary to spend considerable time examining the characteristics of the beams before attempting such measurements. The beam uniformity was examined both by scanning with a small silicon, lithium-drifted, p-i-n detector used in the open circuit voltage mode of operation and by the use of film techniques. It has been found possible to obtain a beam which is of uniform intensity to within 4% over a diameter of approximately 10 cm. In practice, it has been found convenient to accomplish the initial spreading and positioning of the beam by using a television system to observe the beam profile on a scintillating screen. The maximum total output of the 45 MeV beam is

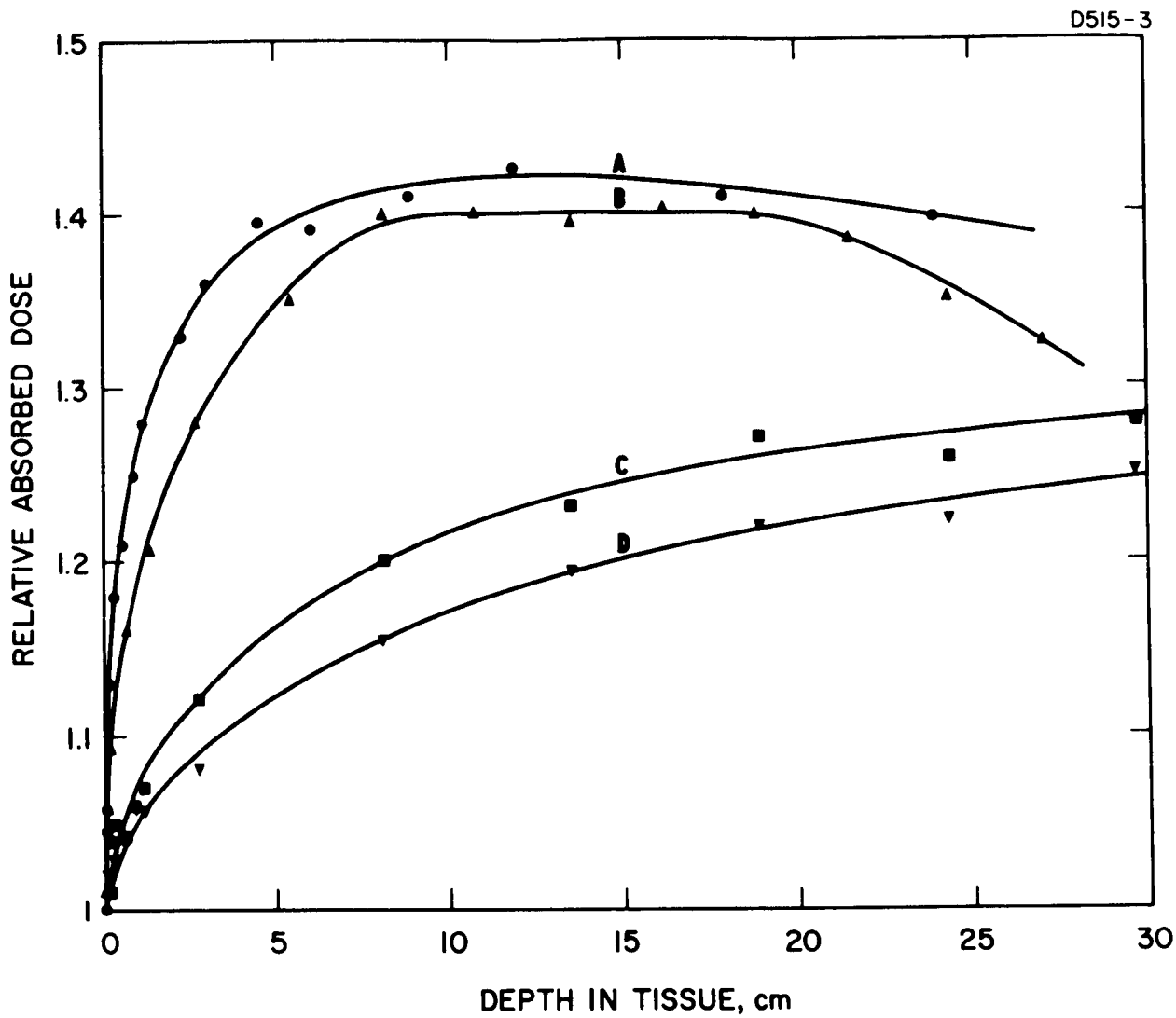

Fig. 1. Center line depth dose distributions for high energy protons. Curve A is for 730 MeV protons, B for 630 MeV protons, C for the 730 MeV beam degraded by 44 in. carbon, and D for the same beam degraded by 10.76 in. copper. The resulting proton energies were 220 MeV and 260 MeV, respectively. To obtain the 630 MeV protons, 10.25 in. carbon was used.

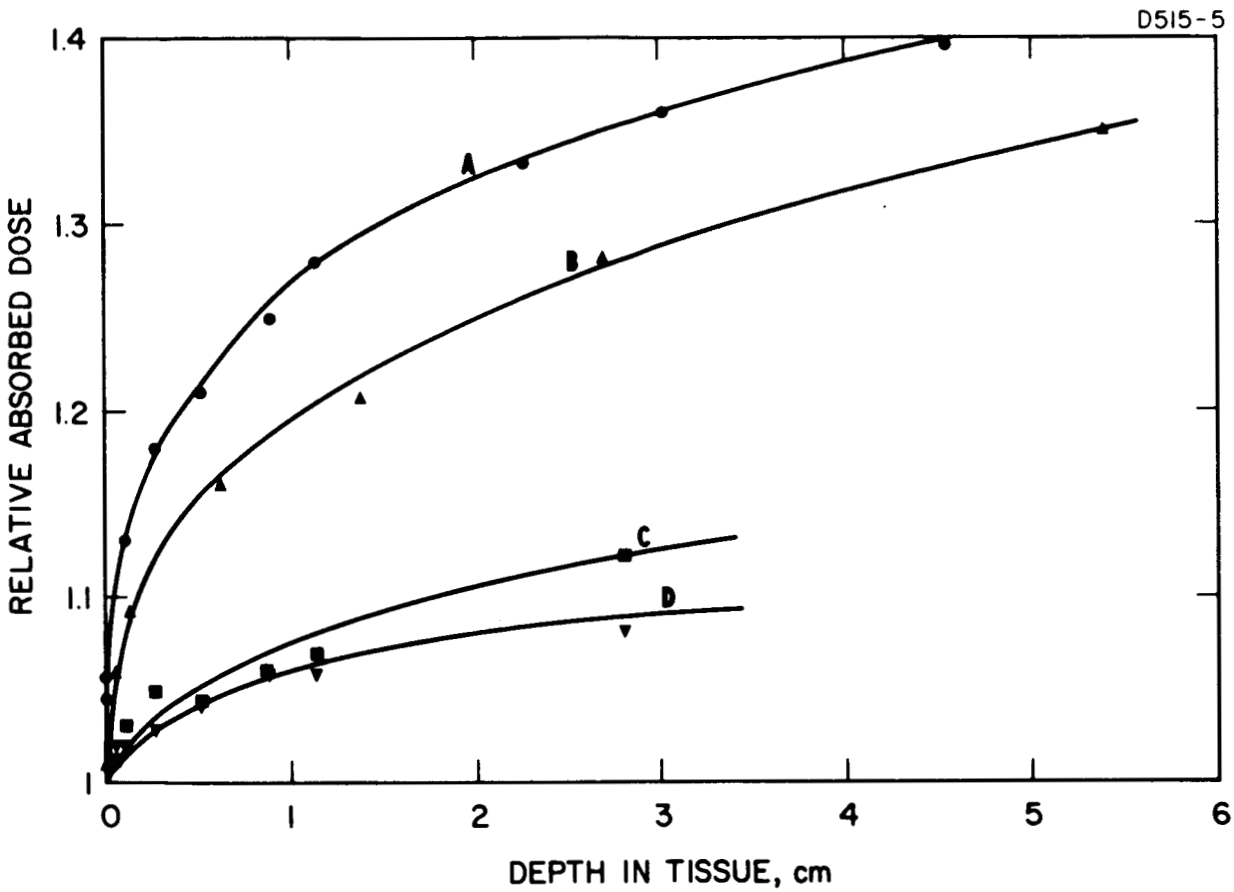

Fig. 2. Initial portion of center line depth dose distributions shown in Fig. 1. Curves are labeled as described in caption of Fig. 1.

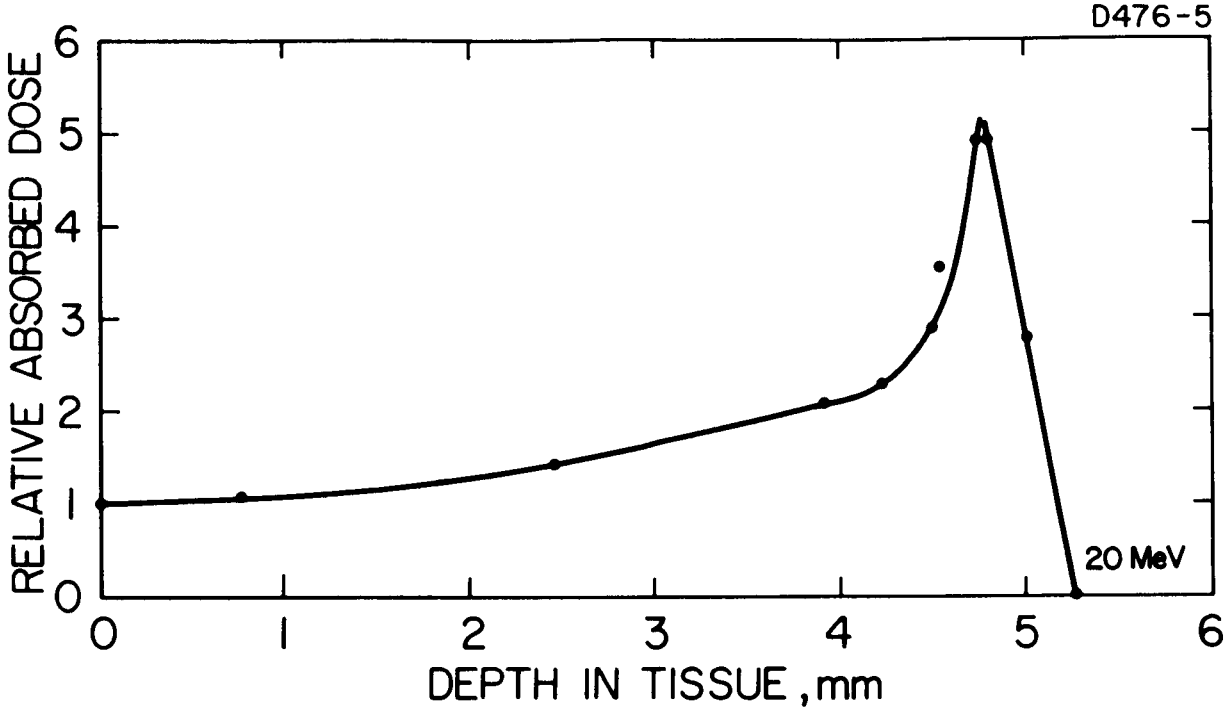

Fig. 3. Center line depth dose distribution for $\simeq$ 20 MeV protons.

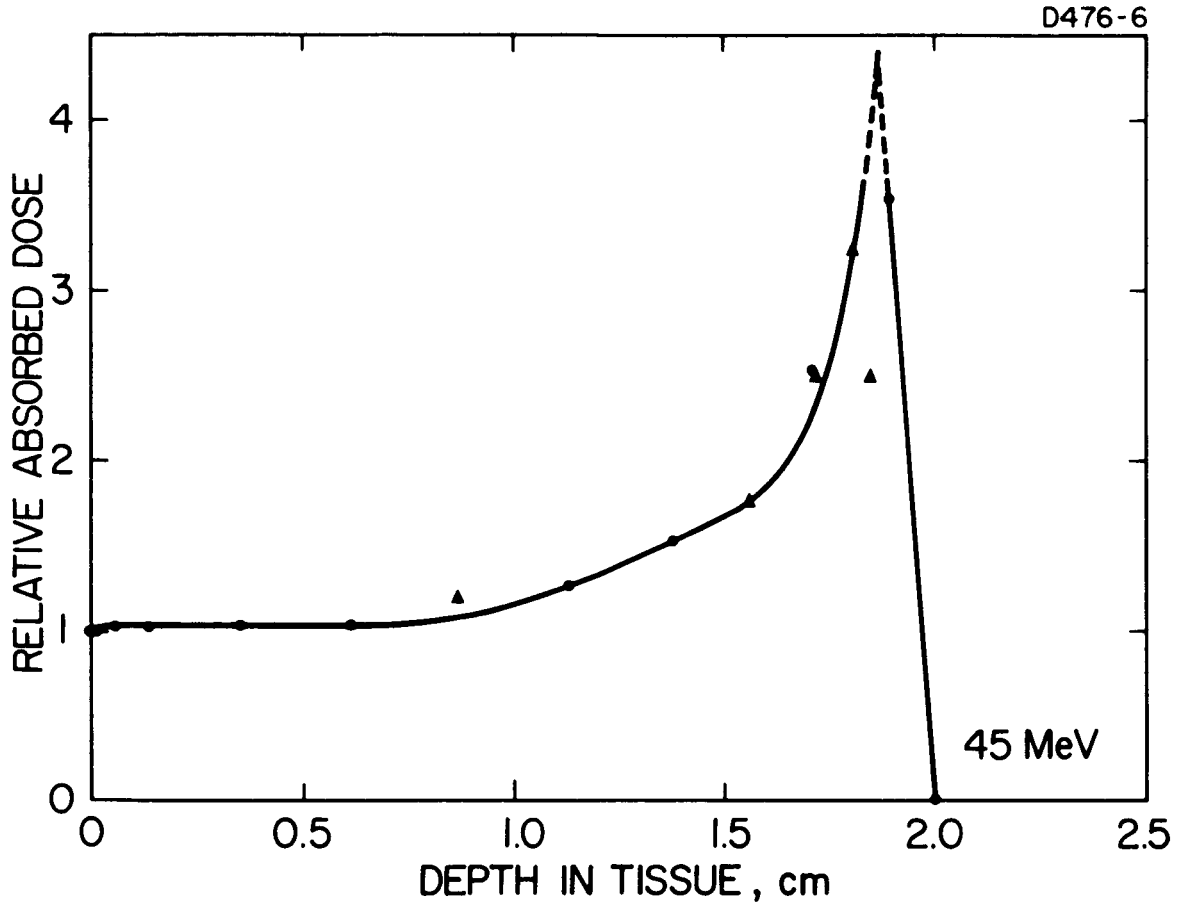

Fig. 4. Center line depth dose distribution for ≃ 45 MeV protons.

10^{12} protons/sec with a FWHM $\cong$ 400 keV, while that of the 20 MeV beam is approximately 5 x 10^{10} protons/sec with a FWHM $\simeq$ 200 keV. The energy of the higher energy beam was actually 46 $\pm$ 0.5 MeV upon emerging from the machine, but an air path of 30 cm reduces the energy of the protons impinging upon the phantom material to about 45 MeV.[6] The lower energy beam emerges from the machine with a nominal energy of 25 MeV, which is reduced to approximately 20 MeV[6] by traversing an air path of 1.9 m before impinging upon the polystyrene phantom material. This 25 MeV beam has a more accurately known energy and a smaller energy spread since it is magnetically deflected. The definite flatness of the 45 MeV center line depth dose distribution observed up to about 6 mm is of considerable practical interest, since it permits accurate dosimetry for biological experiments involving irradiation of tissue cultures, etc., with protons of this energy.

A preliminary experiment was performed to determine the importance of the scatter contribution for the 45 MeV proton beam. This consisted of measuring the surface dose with the extrapolation chamber in the polystyrene phantom for a beam with a diameter of approximately 4 in. A collimator was then imposed which let only a 1 in. diameter beam through. This resulted in approximately a 15% decrease in the surface dose. This figure should not be considered to have too much significance, however, since in this rather crude experiment it is impossible to really determine what part of this result is due to large angle scatter in the phantom material and what part to air scatter. Further work on measurement of side and back scatter will be undertaken.

The center line depth dose distribution for 137 MeV protons, shown in Fig. 5, was determined using the Harvard University 95-inch Synchrocyclotron, which produces protons at an energy of 160 MeV. Since this beam is routinely spread for biological experimentation most of the important parameters for our purposes had been well predetermined. The beam was spread by using multiple-Coulomb scattering in a lead scatterer of 7.64 gm/cm^2, which together with a 360-cm air path attenuated the proton beam to 137 $\pm$ 2 MeV. This scattering produced a broad uniform intensity profile, varying by only 10% over a diameter of 30 cm. This intensity profile was measured using a tiny solid state diode. The dose rates employed were of the order of 50 rads per minute. For purposes of comparison, Fig. 6 shows the peak near the end of the range for the 137 MeV, 45 MeV, and 20 MeV proton beams.

The center line depth dose curves for 220 MeV and 260 MeV protons are shown in Figs. 1 and 2. It may be seen that both of these curves continue to rise for tissue depths up to at least 29 cm and that the curve for 260 MeV protons falls below that for 220 MeV protons, in contrast to the general trend observed at higher energies. This is of considerable interest since the 220 MeV proton beam was obtained by

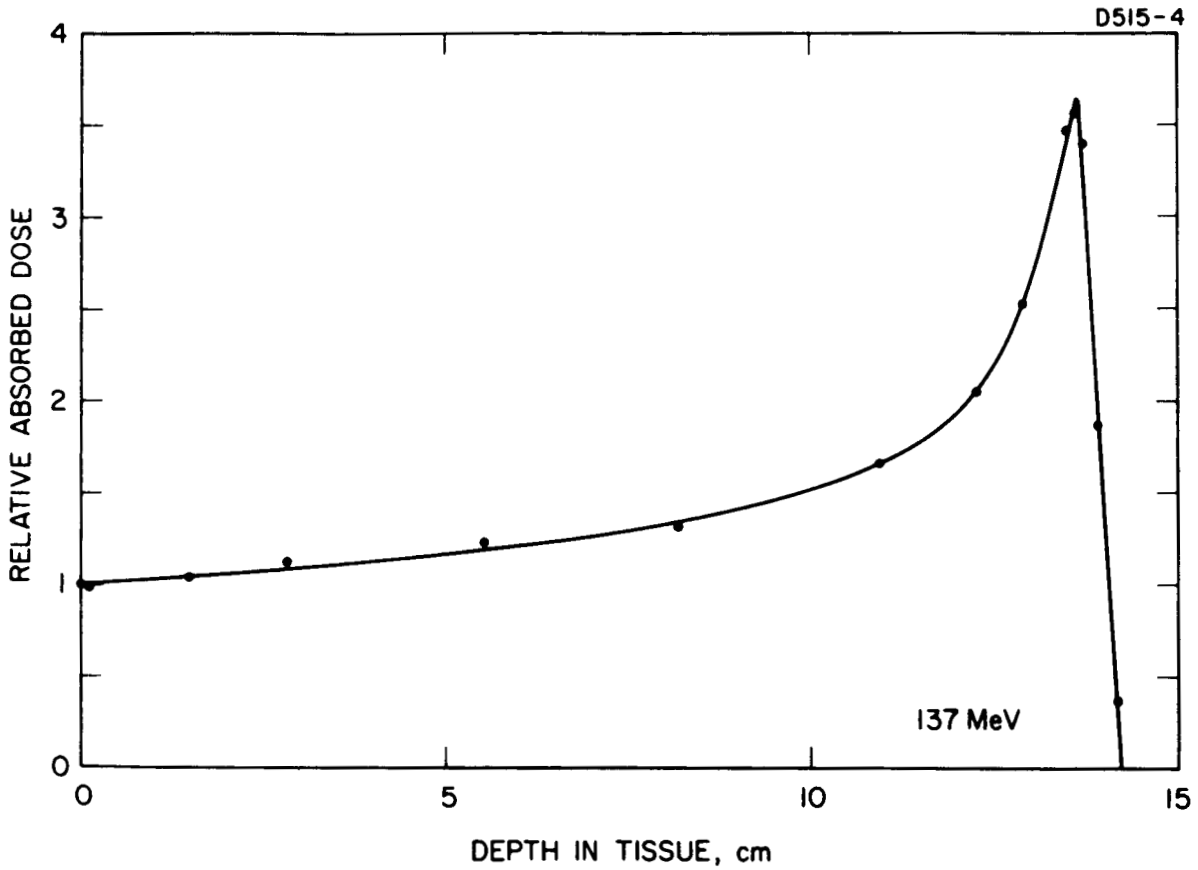

Fig. 5. Center line depth dose distribution for 137 MeV protons.

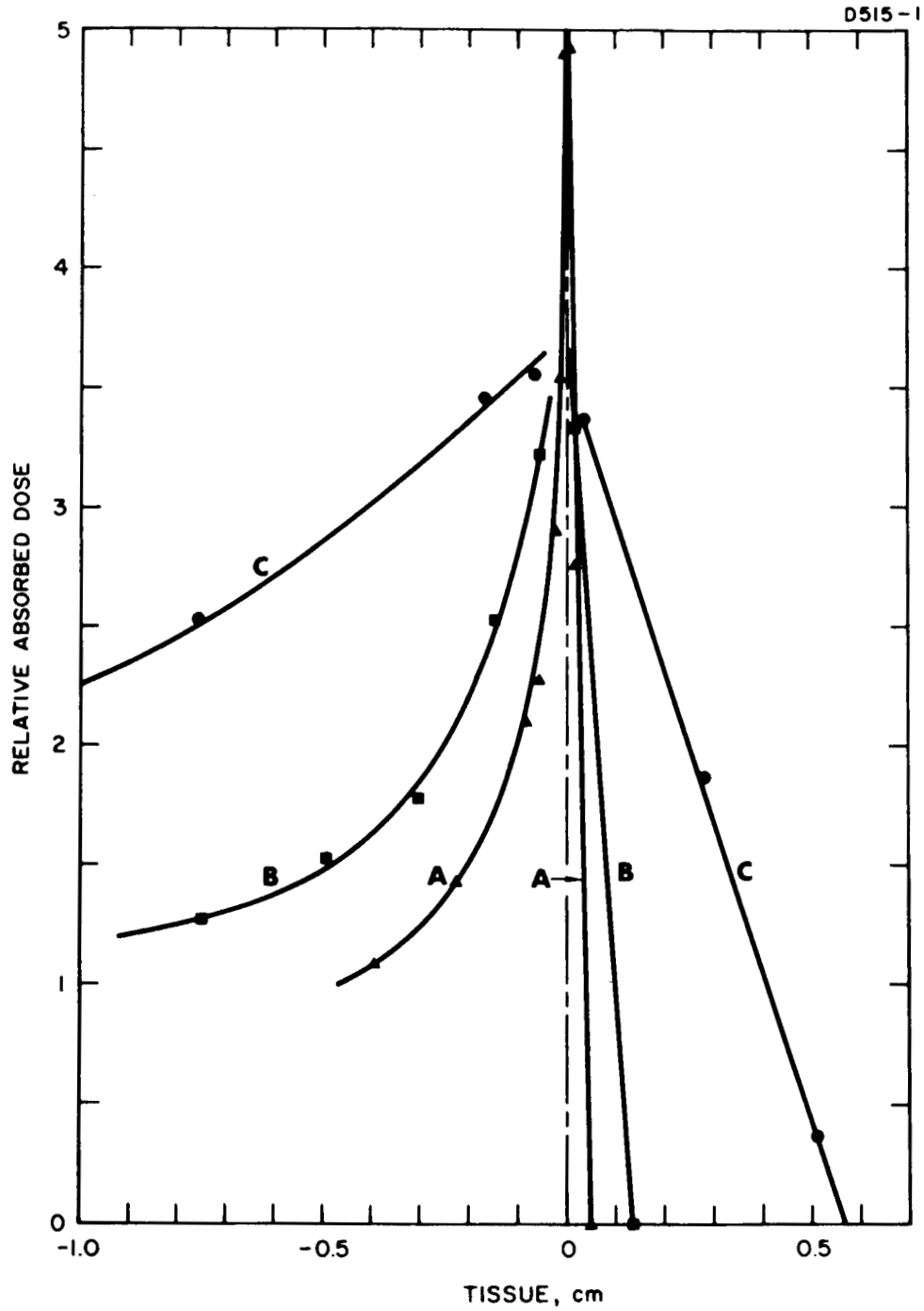

Fig. 6. Expanded peaks in center line depth dose distributions near end of proton ranges. Curves A, B, and C are for proton energies of 20, 45, and 137 MeV, respectively. The curves have been normalized to a common point corresponding to the peak dose rate observed.

degrading the Berkeley 730 MeV beam with 44 in. of carbon (ρ = 1.78) whereas 10.75 in. of copper (ρ = 8.8) was used for degradation to 260 MeV. One might, therefore, assume two things about the resulting beams to explain the observed center line depth dose distributions. First, the continuing rise at large tissue depths may be logically explained by the fact that both of these lower energy proton beams inherently have a much larger percentage of neutron and/or gamma ray contamination than the higher energy beams which is due to nuclear interactions in the degraders. The large mean free path of these high energy radiations would require that a deeper depth of tissue be penetrated before attainment of charged particle equilibrium. Secondly, the percentage of neutrons in the beam after degradation by the copper is considerably greater than that introduced by the carbon. This neutron component leads to a slower build-up of dose with depth of tissue penetrated, since the production of secondaries per unit primary path is less. Considering just these two curves, some of the observed differences could be due to differences in the primary charged particle spectra resulting from degradation by carbon as contrasted to copper resulting in (a) a difference in secondary production per unit path length of the primaries, (b) a difference in the energy distribution of the secondaries, (c) a difference in the angular distribution of the secondaries. A very detailed experimental study would be necessary to determine the exact reasons for the detailed shapes of the observed depth dose distributions.

From the preceeding comments it is obvious that these curves should not be taken to be taken to be center line depth dose distributions for beams of pure 220 MeV and 260 MeV protons. While these curves are certainly of interest for the interpretation of the results of the many biological experiments performed with beams degraded in this manner, they should not be interpreted as center line depth dose distributions which would occur in a biological specimen exposed to fluxes of 220 MeV and 260 MeV protons. Clearly such measurements in this energy range should be done using undegraded proton beams of the desired energy. It is hoped that this may be accomplished in the near future using the 300 MeV proton beam available at the new NASA Langley cyclotron facilities.

An additional very important implication of the observed results is that it is completely inadequate for purposes of manned space flight to merely calculate the theoretical average energy of high energy protons after passing through a given thickness of shielding material and use this value to predict biological effects, since the measurements clearly show that the type of shielding material would significantly affect the resulting center line depth dose distributions in a manner which cannot presently be predicted theoretically. This once again emphasizes the utmost importance of direct experimental measurements of the macroscopic distributions of absorbed dose for high energy protons to supplement and to guide theoretical developments and assumptions in these complex dosimetric problems.

Further study is also needed to determine the relative importance of the different contributions to the total dose for beams of monoenergetic protons. A new extrapolation chamber for this purpose has been built and successfully tested. This chamber is shown in Fig. 7. The chamber is constructed completely of Shonka tissue-equivalent plastic so that the influence of side-scatter can be studied accurately. The chamber has interchangeable back electrodes and guard rings, thus permitting a study of the effect of changing tissue composition (bone-soft tissue, etc.) on absorbed dose. Further study to determine the exit dose patterns and the details of the sidescatter contributions are necessary to make the data applicable to calculations involving complex geometrical situations.

B. Treatment of Data

The raw data obtained using the extrapolation chamber technique consists of the ionization produced current per unit collecting volume extrapolated to zero collecting volume, as a function of depth in a polystyrene phantom. Several factors must be considered in order to convert this data into relative absorbed dose as a function of depth in tissue. The first correction to be applied is to convert depth in polystyrene to an equivalent depth in tissue. The only meaningful way to make such a conversion is obviously on the basis of equal energy losses in the two materials as the primary beam energy is degraded. That is, an increment of depth in tissue is taken as equal to an increment of depth in polystyrene if a proton of the appropriate energy for that depth would, on the average, lose the same amount of energy in passing through each. This conversion was accomplished using proton stopping powers from several different sources for the different energy ranges. The two parameter stopping power tables compiled by Barkas and Berger[6] were used for both tissue and polystyrene when the protons have energies above 2 MeV. Tissue stopping powers below 2 MeV were taken from calculations by Neufeld and Snyder[7] which take into account the partition of energy between excitation and ionization. The values used for polystyrene are those given by Jorgensen.[8]

The conversion of the measured ionization current per unit collecting volume of the extrapolation chamber into absorbed dose in tissue must be done in accordance with the Bragg-Gray principle,[9-13] the basis of all cavity ionization measurements. If a small gas filled cavity is introduced into any medium being traversed by radiation, the Bragg-Gray relationship enables one, if certain necessary conditions are fulfilled, to relate the ionization produced in the cavity to the energy absorbed in the medium. The Bragg-Gray formula is

$$E_m = S_g^m \cdot W_g \cdot J_g$$

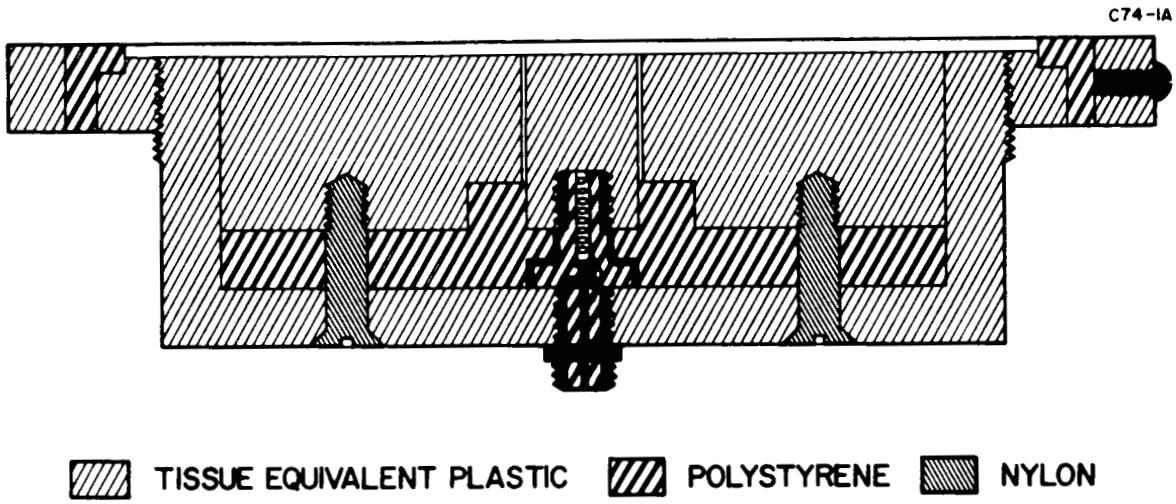

Fig. 7. Tissue-equivalent extrapolation chamber with interchangeable electrodes for studying dose at interfaces where tissue composition changes.

where

E_m = the energy imparted to unit mass of the medium

J_g = the number of ion pairs produced in the cavity gas per unit mass

W_g = the average energy required to produce one ion pair in the cavity gas

S_g^m = the relative mass stopping power of the medium to the gas for the charged particle distribution which exists in the cavity.

The conditions which must be satisfied in order for the Bragg-Gray relation to be applicable are all designed to ensure that introduction of the cavity into the medium does not alter the charged particle flux in the medium. This will be so for charged particles if the following conditions are satisfied:

1. The intensity of the primary radiation is uniform across the cavity.

2. The dimensions of the cavity are small compared to the range of all the charged particles entering the cavity.

3. Essentially all of the ionization produced in the cavity gas is due to charged particles (primary or secondary) originating outside of the cavity. This condition is necessary to ensure that the ionization in the cavity gas is due to the same charged particle spectrum which would exist at that point were the cavity not introduced.

It is implicit in the Bragg-Gray formula that the values of both S_g^m and W_g used must be those corresponding to the particular charged particle spectrum entering the gas filled cavity at the point of measurement. For high energy protons especially careful consideration must be given to the proper value of S to employ, especially in those cases in which the protons are eventually completely stopped in the phantom material. When a high energy proton interacts with matter it initiates a complex spectrum of lower energy secondary particles. According to the mechanism of high energy nuclear reactions of particles with complex nuclei first proposed by Serber,[14] an inelastic collision of a proton with a nucleus produces, by direct interaction with the nuclear

constituents, several secondary nucleons ranging in energy from a large fraction of the incident proton energy down to a few MeV. This leaves a highly excited recoiling nucleus which loses most of its excess energy by evaporating nucleons and heavy particles with energies of a few MeV. It is evident that to follow in detail the change in these spectra as a function of phantom depth and changing primary energy, in order to average the relative mass stopping power values over the charged particle spectrum present at each point in the phantom, would be a tremendously complex if not insoluble problem. Fortunately, however, a sufficiently accurate conversion can probably be made without doing this. A number of computer code calculations of tissue depth dose for high energy protons have recently been published,[15-19] several of which indicate the relative contributions due to primary and secondary (cascade, evaporation, and hydrogen elastically scattered) protons and to heavy evaporation particles and recoil nuclei. These predict that the dose due to all heavy particles is approximately two orders of magnitude below the primary proton dose over the range calculated (up to 400 MeV), and these may thus be ignored completely in this conversion. The dose due to secondary protons is only of the order of a percent of the total dose in the tens of MeV energy range, but becomes more important as the primary proton energy increases. The maximum secondary proton contribution amounts to about 20% of the total dose at 200 MeV[15,16] and reaches 50% at 730 MeV.[19] Thus, for the higher energy curves the secondary proton dose is quite significant, which is, of course, immediately evident from the experimental results at 630 MeV and 730 MeV. However, in converting the present curves it was assumed that since the secondary protons would be spread out over the large energy range from very low energies up to the initial proton energy, and since the relative mass stopping power of tissue to air changes by only a couple of percent from 730 MeV clear down to 10 MeV,[6] the contribution to the dose from secondary protons having a relative mass stopping power much different from the primaries would be very small and could be ignored. Thus, the only conversion considered necessary was that due to the change in S as the primary proton was degraded to very low energies near the end of its range. Below 2 MeV these values were computed using Whaling's values[20] for air and Neufeld and Snyder's values[7] for tissue.

It should be pointed out, however, that further study of this problem has turned up additional data which weaken somewhat the assumption basic to this simplified calculation. These data[21-26] consist of representative energy spectra of both cascade and evaporation protons which have been measured and calculated for various materials and incident proton energies. Although none of these data are specifically for tissue or tissue-like material, they generally show a peaking of the secondary proton spectra at fairly low energies. The degree to which the present curves would be changed by averaging the relative stopping power over such spectra for tissue should certainly be examined.

The other factor in the Bragg-Gray formula which could possibly be energy dependent for protons is W, the average energy required to produce one ion pair in air. The data available from the literature on W for protons are quite meager. The only data directly applicable to air show a difference in W of air of only a few percent for 340 MeV protons[27] and 1.8 MeV protons.[28] In addition, the W for protons has been shown to be constant down to 25 keV in argon[29] and down to 10 keV in hydrogen.[30] In a recent article, Phipps, Boring and Lowry[31] have summarized ionization data for a variety of ions in argon, and have shown a definite systematic increase in W as the velocity of the charged particle decreases below a certain value. Such an increase seems to occur for most gases. The point at which their data show a noticeable increase in W is when the charged particle velocity reaches approximately the velocity of an electron in the first Bohr orbit of hydrogen. This corresponds to an energy of approximately 25 keV for protons. Thus, the best that one can say on the basis of presently available data is that W for protons in air is essentially constant at high energies and probably does not begin to increase noticeably until the proton has reached an energy of a few tens of keV. Therefore, although the W for protons in air probably increases somewhat at very low energies, since there is no experimental data on which to base the value of such a change, and since any such change would at any rate affect only the very last portion of the curves, W was taken to be constant and no correction applied to the center line depth dose measurements.

III. SPHERICAL PROPORTIONAL COUNTERS FOR MICRODOSIMETRY

The second major aspect of the work has been concerned with developing and applying methods for measuring microscopic dose distributions. Such distributions consist not only of absorbed dose, but also of its distribution in energy deposited per event in biologically meaningful volumes. The aim in this phase of the study is to perfect several different types of tissue-equivalent proportional counters which may be used to simulate a wide range of tissue volumes, and to determine the microscopic dose distributions produced by various radiations in these simulated volumes. Such distributions will, in turn, be used to evaluate and analyze the distributions obtained in small, spherical solid state detectors. In order to obtain meaningful microscopic dose distributions, however, both the collection efficiency and the gas multiplication must be uniform at all operating gas pressures and collecting voltages for pulses formed by particles passing through any portion of the chamber volume. A great deal of effort has gone into rigorous and definitive examinations of these characteristics in an attempt to perfect an optimum electrode design. These properties have been explored using a brass chamber simulating the electrode and collecting volume of the tissue-equivalent chambers in conjunction with alpha sources, as well as with the tissue-equivalent chambers themselves using high energy proton beams.

The Shonka-type tissue-equivalent plastic used in the walls of the chambers consists essentially of a mixture of polyethylene, nylon, carbon, CaF_2 and SiO_2. In order to meaningfully study energy transfer patterns due to charged particles in simulated microscopic tissue volumes requires tissue-equivalence in the gas-collecting volume as well as in the chamber walls. For measurement of non-nuclear charged-particle interactions it is sufficient to simulate the electron density of tissue, in contrast to the more complicated simulation required for measuring photon interactions in which the cross sections for photoelectric, Compton, and pair production processes must all be taken into account or in the case of particles where nuclear interactions are important. The electron density of ICRU tissue[32] is 3.31×10^{23} electrons/g, and it is possible to match this density quite well with gas compositions which are well behaved in the proportional counting region. A commonly used counter gas is methane, with an electron density of 3.77×10^{23} electrons/g, and this gas was used in the pioneering experiments of Rossi.[1-5] However, early work at this laboratory showed that decomposition of methane resulted in very poor sealed counter stability. The gas used in the present chambers consists of an equimolar mixture of helium and carbon dioxide, which had previously been successfully used by Caswell.[33] Both constituents of this mixture are quite stable to ionizing radiation and the mixture performs very well in the proportional region. Because the electron density of both helium and carbon dioxide

is about 3.01×10^{23} electrons/g, it is impossible to match the electron density of the tissue-equivalent walls exactly. However, the discrepancy for this mixture is no worse (although in the opposite direction) than that of the methane filling used by Rossi.

A study of chamber resolution (FWHM) in the brass chamber as a function of operating voltage and gas pressure resulted in some rather disturbing results, which were the first indications that the electrode design initially used in this program was deficient. Using a collecting potential of 800 V, the resolution of the peak due to a collimated α-source directed across the diameter of the chamber was examined from 0.60 cm Hg pressure to 8.00 cm Hg pressure. At pressures from 0.60 cm Hg to 2.00 cm Hg, the normal operating pressure of the tissue-equivalent chamber, the resolution improved almost exactly as would be expected from the statistics of the interaction process.[34] However, as the pressure was increased above 2.00 cm Hg the resolution continuously deteriorated, reaching a value of 60% at 8.0 cm Hg. In addition, at each pressure investigated the resolution deteriorated with an increase in voltage.

Similar indications of serious collection problems at extremes of pressures and collecting voltages were observed by examining the response to an uncollimated alpha source located on the wall of the chamber. Rossi has shown[1] that a spherical proportional counter with a monoenergetic source located on the surface of the sphere should give a rectangular pulse height spectrum. The spectra for the initial electrode configuration were examined over a range of pressures and voltages. Apparently satisfactory uniformity of volume response was observed at 2.0 cm Hg pressure over a range of voltages from 850 V to 920 V. A typical example is shown in Fig. 8. However, raising the voltage to 950 V completely destroyed the rectangular pulse height spectrum. Likewise, changing the pressure much below or above 2.00 cm Hg destroyed the rectangular spectrum, and this could not be restored by changing the voltage. It should be pointed out however, that extreme caution must be used in interpreting the results of tests of uniformity of volume response using this rectangular pulse height spectrum. As will be detailed presently, the initial electrode design was found to suffer from incomplete charge collection and several new designs have been studied. An initial attempt at this type of test with a new electrode structure produced a very distorted spectrum which, however, turned out to be caused by a new source used in the test rather than the electrode configuration, since substitution of the formerly used source produced a very good rectangular spectrum. The problem was evidently caused by rather severe self-shielding of short path lengths due to non-uniform source plating. Since this type of spectrum is thus seen to be so dependent upon the source characteristics it is obvious that there is

M 4383

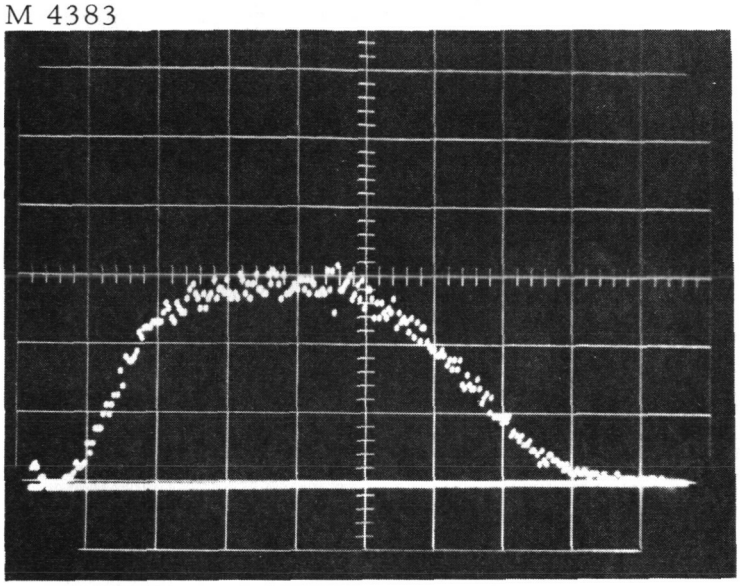

Fig. 8.
Response to an uncollimated polonium-210 α-ray source located on the wall of a spherical proportional counter operated at a potential of 875 V and a gas pressure of 2.00 cm Hg. Each division on the abscissa represents 51.2 channels with zero energy corresponding to channel No. -5. The ordinate is a linear display.

a very real chance of misinterpretation of this test, making it of dubious value for quantitative testing. Also, it is readily seen that the test is not sufficient since this spectrum can be obtained even without complete charge collection.

The explorations of uniformity of collection and multiplication undertaken using the tissue-equivalent counters in the UCLA proton beam were done by using a small frontal area silicon lithium-drifted, p-i-n detector in coincidence with the chamber to select a portion of the proportional counter sensitive volume for examination. It was mentioned in the previous summary technical report that an effect then thought to be due to an interaction between the protons and the walls of the tissue-equivalent chamber had prevented the accumulation of coincidence spectra in the new experimental area. A study of this problem has shown that, in fact, no such interaction occurs and that the apparent effect was due to the normal scattering pattern of protons from the polyethylene target generally used in the cyclotron. In protons scattered from a target containing carbon and hydrogen there are normally a number of proton energy peaks produced, the most prominent at the angle of our experiment being those due to elastic scatter from hydrogen and carbon. The energy of the proton peak due to elastic scatter from carbon does not vary much with angle of scatter while the energy due to elastic scatter from hydrogen does. On the other hand, while the intensity of the hydrogen elastically scattered peak dues not vary with angle the intensity of the carbon elastically scattered peak is a very strong functionof angle, decreasing very rapidly with increasing angle at the position of our experimental set-up. Thus, when the p-i-n detector was remotely moved 2.5 cm from a point to the side of the proportional counter to directly behind it, it was also moved to a scattering angle several degrees smaller, leading to a large decrease in the ratio of the intensity of the carbon scattered peak to that of the lower energy hydrogen scattered peak which appeared to be caused by an interaction in the chamber walls. With this understanding of the scattering pattern it was a simple matter to arrange the experimental parameters to obtain additional useful data using this coincidence method. This complication was entirely eliminated in much of the experimentation by being able to obtain our own beam time and thus use a pure carbon target. This also made it practical to obtain much better statistics, since use of a somewhat thicker target than normally employed when we were in a satellite position, in conjunction with a move to a smaller scattering angle, greatly increased the count rate obtainable.

It should be pointed out that properties of the interaction of high energy protons with matter such as this markedly anistropic scattering from carbon are of considerable significance to consideration of microscopic energy transfer patterns. While an interaction such as this would have little effect on the macroscopic properties such as center line depth dose it could obviously greatly influence the absorbed energy density on a microscopic scale and should be carefully taken into account in any such considerations.

Several attempts to collect coincidence spectra were made, with varying degrees of success. It was finally determined that the upper limit of proton flux with which the counter could be successfully operated was approximately 3000 protons/cm^2/sec. Above this value the coincidence spectrum was completely obliterated, presumably due to pulse pileup and space charge effects. This is shown very dramatically by Figs. 9 and 10 which show coincidence spectra for fluxes of approximately 9000 protons/cm^2/sec and 3000 protons/cm^2/sec, respectively. The shape of the coincidence spectrum in Fig. 10 should be noted. The high energy tail is characteristic of spectra in which the average energy loss is much less than the maximum possible energy loss per collision, and is described by the theory developed by Landau[35] and Symon.[36,37]

With all of these parameters understood it was possible to extend the study of the uniformity of response in different parts of the chamber. Initially this consisted of simply selecting different paths through the tissue-equivalent chamber by moving the silicon p-i-n detector to various positions behind it. In this manner coincidence peaks were observed at 1 cm to the side of the center of the chamber, but could not be observed at 2 cm to the side or 1 cm up from the center. In these positions the rate of collection of the coincidence spectra decreased drastically and the resulting spectra were identical in shape to the ungated whole counter response. It was thus obvious that in these cases the spectra represented nothing but random accidental coincidences. However, it was also realized that it was not necessary to conclude from this alone that the chamber was not collecting from these areas. Another possibility which had to be explored was that for pulses formed far from the center electrode the transit time of the initial electrons to the center electrode was such that the gate had already closed before the pulse produced by them reached the analyzer. The maximum electron transit time is an exceedingly difficult value to estimate, especially with the initial electrode design. This was therefore studied experimentally by introducing a variable delay gate generator in the line carrying the gating pulse. However, variation of the gate delay time and gate width over a wide range did not permit accumulation of a coincidence peak in the outer portions of the sensitive volume, indicating poor collection efficiency. It should also be noted in this connection that the pulse height of the coincidence peak collected at 1 cm to the side of center was considerably smaller relative to that through the center than can be explained on the basis of relative path lengths, again indicating poor collection efficiency.

It might be mentioned that in the course of the experiment described above, the various circuit parameters involved in recording the pulse height distributions generated in the spherical sensitive volume were examined in some detail. One change which resulted was to increase the clipping time in the amplifier, changing the total pulse

M 4379

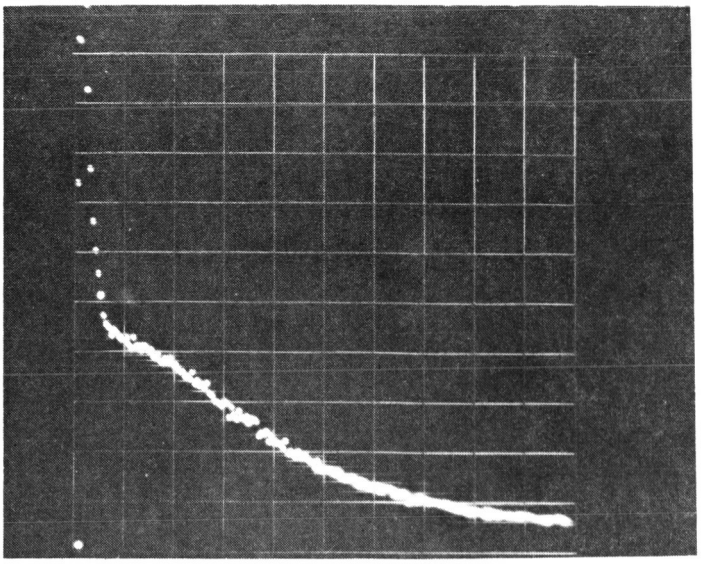

Fig. 9.
Response of a 2 in. spherical tissue-equivalent proportional counter to traversal of a diameter by 46.5 MeV protons, with a proton flux of approximately 9000 protons/cm^2/sec. Each division on the abscissa represents 20 channels, with zero energy corresponding to channel zero. The ordinate is a linear display.

M 4378

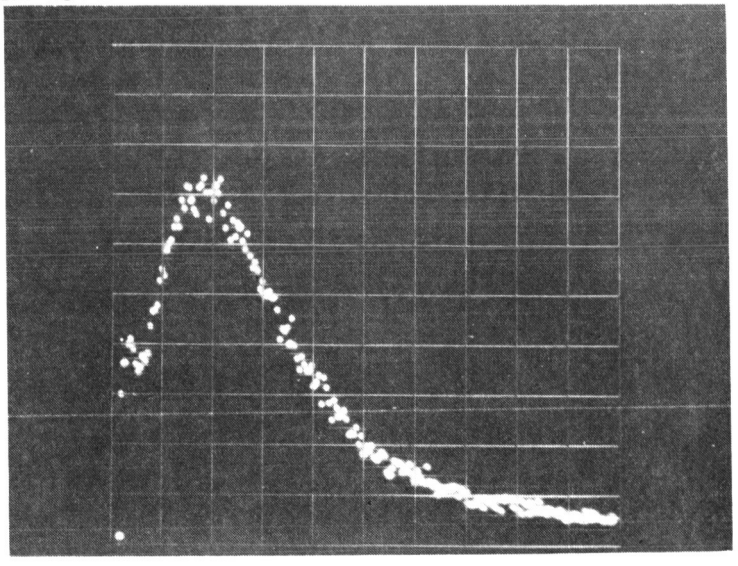

Fig. 10.
Response of a 2 in. spherical tissue-equivalent proportional counter to traversal of a diameter by 46.5 MeV protons, with a proton flux of approximately 3000 protons/cm^2/sec. Each division on the abscissa represents 20 channels, with zero energy corresponding to channel zero. The ordinate is a linear display.

length from 3-4 μsec to approximately 15 μsec. This was done to insure that the pulses were not being electronically clipped at a time less than or approximately equal to the collection time of those electrons having to make the longest traversal within the counter. If this were so it would imply, first, that the pulse height for an individual pulse would depend upon the position and orientation of its individual track, thus distorting the entire pulse height spectrum and, second, that the pulses were being clipped before reaching full pulse height so that increasing the clipping time would result in an increase in the obtainable signal to noise ratio. Increasing the clipping time did, indeed, increase the observed signal to noise ratio by a factor of about 3 times.

In view of the results indicating poor collection of proton produced pulses in the tissue-equivalent chamber, it was necessary to establish the reason for this deficiency. Two lines of investigation have shown rather conclusively that the poor collection efficiency observed is the result of a deficient electrode design rather than a property of the He-CO_2 gas mixture being used. First, when methane was substituted for the He-CO_2 mixture and the polonium-210 α-ray spectrum resolution observed as a function of pressure and voltage in the brass chamber, the same deterioration of spectrum resolution was observed at extremes of pressure and voltage as in the case of the He-CO_2 mixture. Secondly, a series of examinations were made of the saturation characteristics of the chambers, using a number of different electrodes and for both x-rays and protons. This was done by using the counters as ionization chambers and measuring the current as a function of applied potential for a constant radiation intensity. Saturation was initially attempted in the 46 MeV proton beam using the He-CO_2 gas mixture at 2.0 cm Hg pressure, but was not achieved. In order to determine whether saturation was being achieved in some portion of the chamber near the center and if so to attempt to map that portion of the chamber, a collimator was used in the proton beam to expose only a given portion of the chamber at a time. Since a proton beam through any portion of the frontal area of the spherical chamber produces electron-ion pairs along a complete diameter or chord, complete saturation would not, of course, be expected in this case if it was not achieved for the whole chamber. However, for a given radiation intensity one would expect to see a change in slope of the current versus voltage curve, with a closer approach to saturation being achieved in portions of the chamber in which a better field distribution existed. However, no closer approach to saturation was achieved with the beam collimated through the center than had been achieved with the whole counter.

The possibility was then considered that multiplication might be beginning at the tip of the electrode at low enough voltages that it was preventing the leveling off of the current versus voltage curve which is the normal criterion for showing collection from the complete

sensitive volume. This possibility was examined using the chamber filled with air at atmospheric pressure, which has often been used in proportional counters, and using x-rays as the ionizing radiation. All of the subsequent work using x-rays was done using 140 KVP x-rays filtered with 1 mm Al + 1/4 mm Cu, a current of 5 ma, and a target to detector distance of 20 cm. The first unsuccessful attempt to improve the field distribution was to round the pointed end of the electrode. The next step was to coat the alumina base in which the electrode is supported with aquadag to connect its entire outer surface electrically to the center collector. Although saturation was still not achieved this step provided very good additional evidence of poor collection with the normal electrode configuration, since it resulted in approximately a threefold increase in current at any given voltage. The current again increased slightly, although saturation was still not achieved, when a 1/16 in. diameter steel rod was used as an electrode. Saturation was finally achieved when a 1/4 in. diameter sphere was used in the center of the spherical collecting volume. Saturation then occurred at about 400 V. At lower voltages there was a considerable increase in current over any of the other electrode configurations. Even though multiplication cannot be achieved with this configuration it is still of considerable interest since in a standard geometry the extent to which the current from any new electrode design approaches that of the spherical electrode can be used as a measure of the completeness of collection even if multiplication should begin before saturation can be exhibited in the usual manner.

With recognition of the initial electrode design deficiencies it was necessary to begin a study to perfect a new electrode. However, in view of the fact that the initial electrode design turned out to have poor collection properties even though its uniformity of volume response had appeared quite acceptable using the angled alpha source as a probe in the brass test chamber, it became obvious that a much more definitive test was needed to evaluate any new electrode designs. The brass test chamber has thus been altered to permit a much more thorough examination of the uniformity of volume response using a collimated alpha source or monoenergetic electrons from the β-ray spectrometer. The new design permits a collimated beam to be directed along seven different parallel paths, consisting of a path through the center and three pairs of paths at 1 cm and 2 cm from the center, each subsequent pair being rotated 45°, thus completely mapping one quadrant of the spherical volume. This method of initial testing is thus completely analogous to the test which must ultimately be performed using the tissue-equivalent chamber in the UCLA proton beam. When this testing procedure was used to examine the initial electrode it showed very clearly the very non-uniform volume response inherent in this design.

Tests have been carried out, using the brass test chamber, on a number of new electrode designs. All of these designs have involved a very small diameter wire stretched completely across the spherical volume. One design attempted was an approximation to a design reported in the literature by Benjamin, et al[38] and reputed to give very good uniformity of volume response. However, using a close approximation to the parameters specified by Benjamin for a chamber with a 2-in. diameter we were initially unable even to obtain a peak through the center. By applying an intermediate voltage on the field-shaping electrode included at the ends of the wires in all of the new designs studied, it was possible to obtain peaks in all source positions but no field-shaping voltage was found which gave a satisfactory uniformity of volume response. This design was thus dropped. All of the other design changes tested consisted of variations in the wire diameter, variations of the voltage applied to the field shaping electrodes at the ends of the wire, and modifications to the physical structure of the wire supports.

A 0.003 in. stainless steel wire stretched completely across the chamber volume has been found to give considerably improved performance. First of all, saturation of this electrode in the brass test chamber was shown, using air at atmospheric pressure and the x-ray conditions specified above for the previous saturation tests. Saturation occurred at about 500 V as compared to about 400 V for the 1/4 in. diameter steel sphere and, of course, at the same current level from the chamber. The gain and resolution as a function of voltage for a collimated alpha beam directed across a diameter was studied at a constant pressure of 2.0 cm Hg. No change in resolution as a function of voltage was observed over the range of voltages examined (900-1075 V). The relative gas gain as a function of voltage is seen in Fig. 11. It was noted in comparing these gain figures on an absolute basis with previous values obtained with the initial electrode design that the gain of the 3 mil wire at 900 V and 2.0 cm Hg pressure was only about a fifth of that of the previous electrode for the same parameters. Since for these conditions the peak previously seen from 45 MeV protons in the tissue-equivalent chamber using the coincidence set-up was only about 2-3 times noise, it was imperative that it be possible to make up at least this factor of five by increasing the voltage. This was found to be possible since the new electrode structure permits considerably higher applied voltages before breakdown. It may be seen from Fig. 11 that the gain at 1050 V is more than six times that at 900 V. Since a signal of at least this magnitude must also be obtained at any other operating pressure without adversely affecting other operating characteristics, the pressure was varied over a wide range and the voltage at each pressure increased to insure that the resultant signal output was at least as large as obtained at 1050 V and 2.0 cm Hg pressure. The resolution was examined at each pressure under these conditions and showed a considerable improvement over the old electrode structure. As mentioned previously, the peak resolution using the initial electrode configuration had the very

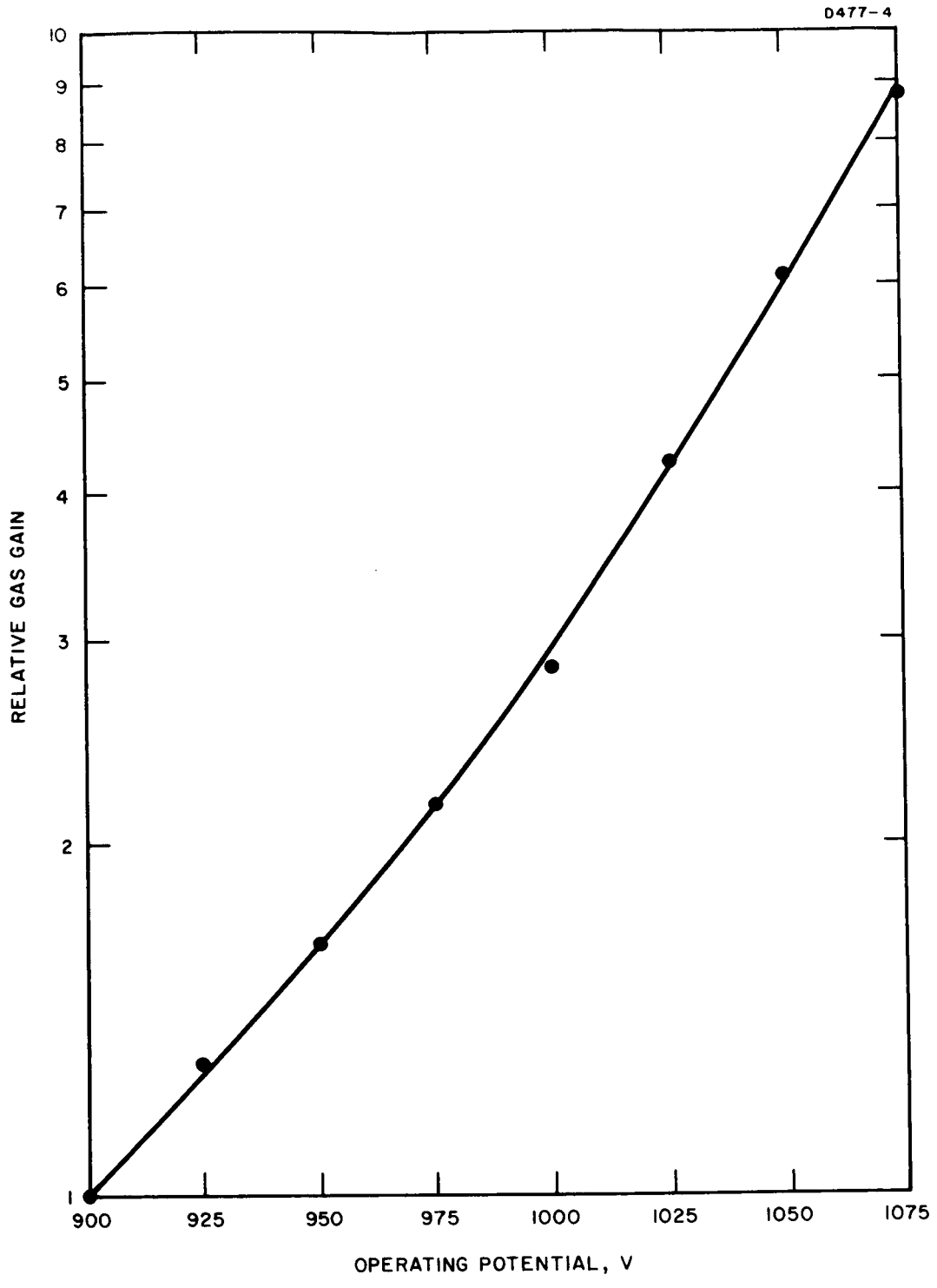

Fig. 11. Relative gas gain as a function of applied potential at 2.0 cm Hg pressure for 0.003 in. stainless steel wire electrode extending across entire chamber.

undesirable property of deteriorating increasingly as the pressure was raised above 2.0 cm Hg, reaching 60% at only 8.0 cm Hg. In contrast, the new configuration exhibited a resolution of about 15% at 10 cm Hg and 18% at 20 cm Hg. The resolution at these higher pressures could not be improved by increasing the voltage further. Only about 2% of the increase in resolution over what would be expected at a pressure of 20 cm Hg can be explained on the basis of a change of stopping power over the greater effective path. Since the resolution should get increasingly better as more energy is left in the chamber this is probably still not an optimum design, but it is certainly a great improvement over the initial design performance and appears to be quite usable over a wide range of pressures.

The design now considered to be optimum and presently undergoing more extensive testing, consists of a 0.003-in. diameter stainless steel wire stretched completely across the chamber diameter with a voltage on the field shaping electrodes which is 30% of the operating voltage on the center electrode. Figure 12 shows the uniformity of volume response obtained with these parameters when operating at a pressure of 2.0 cm Hg. The figures indicated are the ratios of the pulse heights observed to the pulse heights expected for each path length. It will be seen that all points are within 8% of the expected values. It should be pointed out, however, that the resolution of the alpha peak is rather poor in the outer portion of the chamber. Whereas a resolution of about 30% would be expected due to the shorter path lengths, the observed resolutions were about 42% at F and G and 100% at position E, near the end of the center electrode. With no voltage applied to the field shaping electrodes, which of course results in poor uniformity of volume response, the resolution at these points is, indeed, about 30%.

An attempt was made to determine the reason for this poor resolution at the extremities, especially position E. It was hypothesized that part of the reason for the poor resolution might be due to part of each pulse being collected by the field shaping electrodes when positive voltage is applied to them. To test this, the brass chamber was used as an ionization chamber and exposed to x-rays. After a saturating voltage was found with no voltage on the field shaping electrodes, voltage was applied to these electrodes and the current re-examined to see if there was a decrease. The center of the chamber was shielded during this test to give increased sensitivity to conditions at the ends. No decrease was observed, however, indicating that this is not the reason for the poor resolution, which must be due simply to a limited non-uniform field region near the ends of the electrode. It should be pointed out that although this resolution is a large percentage increase in the case of the alpha particle test pulse which has an inherent resolution near 20%, when one is measuring pulses from particles leaving much less energy in the sensor and hence with much larger inherent resolutions, and in only a small portion of the entire volume, this degree of counter resolution is not a serious problem.

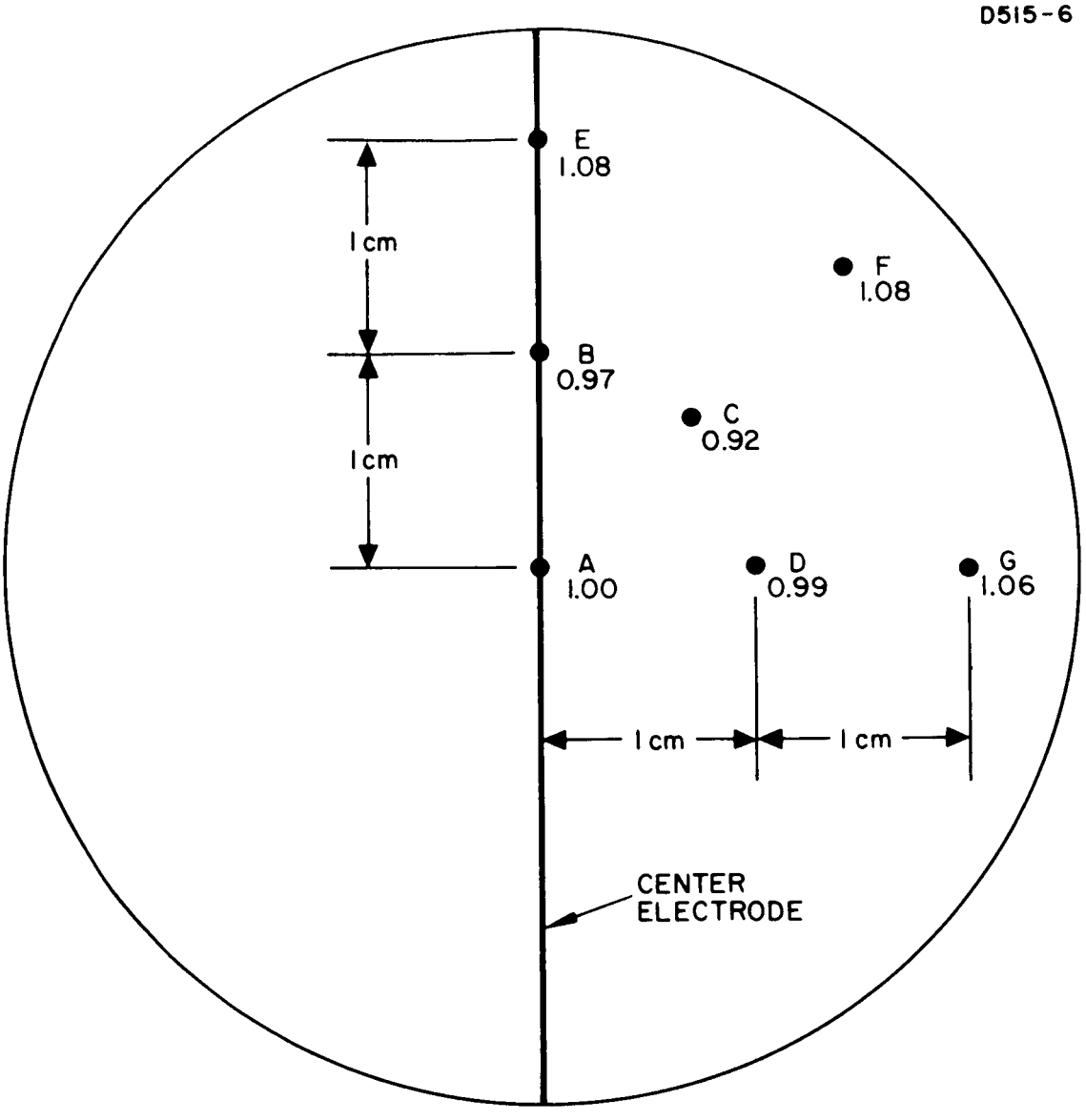

Fig. 12. Volume response of 0.003 in. electrode operated at 2.00 cm Hg pressure, with 1075 V on the center electrode, and 316 V on the field shaping electrodes. Values plotted are the ratios of experimental to theoretical pulse heights for the various path lengths.

IV. SPHERICAL SILICON Au-i-Al DETECTORS

Tiny, spherical, silicon Au-i-Al detectors are of interest since such detectors may be used to obtain information on absorbed dose and for studies of energy event distributions due to high energy radiations in anatomical situations in which the use of proportional counters is impossible due to their much larger inherent physical size. They may also be used in other geometries to investigate the microdosimetric distribution at bone-tissue interfaces, etc., and for situations in which it is desired to simulate larger tissue volumes than is possible with proportional counters.

It was previously reported that a satisfactory method had been developed for fabrication of such spheres from lithium compensated silicon. However, detailed testing showed that the earlier samples suffered from lack of complete collection of radiation generated charge from all regions of the detector volume and were not stable to long storage. Such tests of uniformity of response involve probing around the sphere from pole to pole with the conversion electrons from a very tiny Sn^{113} source. In order to obtain satisfactory spheres it was necessary to carry out a rather extensive study of the field distribution existing within lithium compensated silicon devices after various fabrication techniques. These studies include surface probing by means of a high impedance electrometer circuit, the use of a helium-neon laser beam to study carrier collection efficiency, and capacitance-voltage relationships as a function of frequency.

This study has led to a satisfactory method for preparation of the required detectors. Thick (7 mm) wafers of 200 ohm-cm, p-type silicon are compensated with lithium by diffusion and pulse-drifting in an oil bath. To achieve a uniform field distribution within the compensated material it is necessary to store the devices at room temperature under fairly high bias conditions for periods of about one week. Residual n^+ and p regions are then cut off and the remaining intrinsic region cut into cubes. The cubes are then reduced to small spheres by air abrasion. After etching the surface in nitric-hydrofluoric acid etch, gold and aluminum wires are attached by ultrasonic bonding. Circular masks with diameters less than that of the sphere are used to permit vacuum evaporation of a thin (50-100 Å) gold electrode over the gold wire and a thin aluminum electrode evaporated over the aluminum wire in the same manner, leaving a complete band of uncoated silicon between the electrodes. Units have been achieved which have exhibited noise broadening of an electrical pulser peak (FWHM) of about 8 keV at room temperature. This permits very good spectral resolution, as can be seen in Fig. 13, which clearly shows the K (364 keV) and L_I (388 keV) conversion electron lines from Sn^{113}. These units have also shown good stability under storage. Spectra due to high energy incident radiations obtained with these spherical detectors must be evaluated in terms of the spectra obtained with spherical proportional counters. Data of this type have not thus far been obtained.

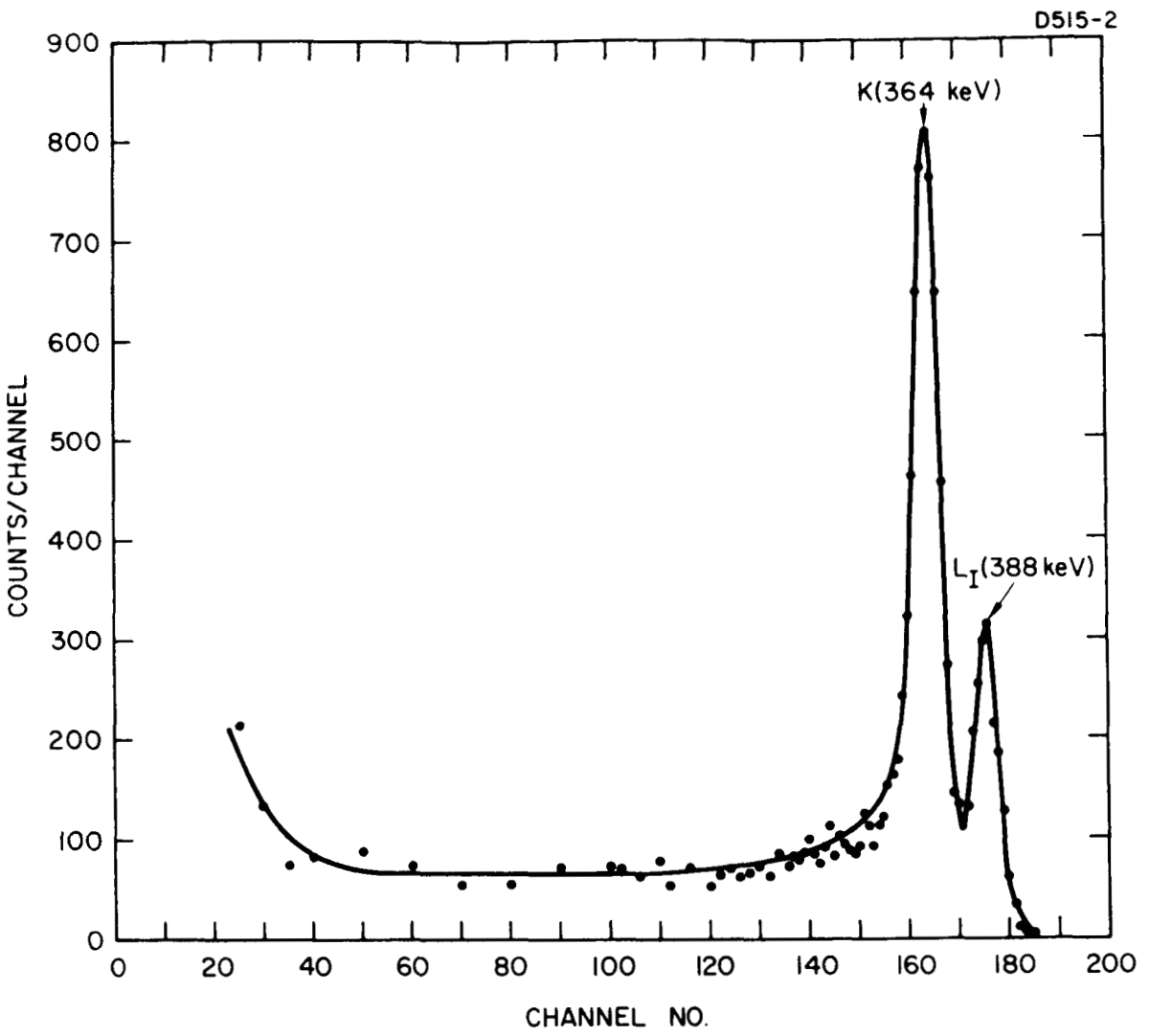

Fig. 13. Response of a 1 mm diameter, spherical, silicon Au-i-Al detector to K and L_I conversion electrons from a Sn^{113} source. Resolution (FWHM) of K line is $\simeq$ 14 keV. Each channel represents 2.1 keV, with zero energy falling in channel zero.

V. CONCLUSIONS AND RECOMMENDATIONS

The measurements thus far completed of the center line depth dose distributions for high energy protons, which were designed to elucidate the distribution of absorbed dose on a macroscopic scale, have shown some very significant and previously unpredicted features. The very rapid initial rise of absorbed dose with tissue depth is obviously of considerable practical importance particularly with respect to small animal irradiations. In addition, it points to the definite importance of the contribution of the secondary charged particles, resulting from nuclear interaction processes, to the absorbed dose at very high primary proton energies. The shapes of the center line depth dose distributions for proton energies up to 140 MeV, on the other hand, indicate that secondary production is relatively unimportant in this lower energy range. It would obviously be of great interest to obtain center line depth dose distributions for protons with energies intermediate between 140 MeV and 630 MeV. It is planned to accomplish this early in the next quarter, using the 300 MeV and 600 MeV proton beams available at the new NASA Langley cyclotron facility.

The significance of the center line depth dose distributions observed for the severely degraded proton beams (220 MeV and 260 MeV) should be pointed out. A very important implication of the observed results is that it is completely inadequate for purposes of manned space flights to merely calculate the theoretical average energy of high energy protons after passing through a given thickness of shielding material and use this value to predict dose or biological effects, since the results clearly show that the type of shielding material would significantly affect the resulting center line depth dose distribution. This once again emphasizes the importance of direct experimental measurements of the macroscopic distributions of absorbed dose for high energy protons to supplement and to guide theoretical developments in these complex dosimetric problems. Further study to determine the importance of side- and back-scatter contributions and possibly to examine the exit dose patterns for the higher energy beams would be of interest, since this information would be helpful in applying the data to calculations involving biologically complex geometrical situations. The information thus far obtained in this phase of the study is felt to be of considerable significance, bringing to light, as it does, a previously unpredicted feature of the depth dose distributions which is of great practical and theoretical importance as well as contributing to the basic knowledge of the interactions of high energy protons with matter.

In the area of the development of a satisfactory proportional counter for microdosimetric measurements, the operating characteristics of the 0.003 in. stainless steel electrode will be examined in detail. The resolution and uniformity of volume response will be studied

in the brass test chamber over a range of gas pressures and operating voltages, using the improved scheme for scanning portions of the chamber with a collimated beam. This phase of the study should also be extended to the determination of the response characteristics for minimum ionizing particles, and calibration for low energy electrons such as those which will be present as delta rays in the tissue-equivalent chambers during actual proton energy event size studies. This can be done in the same brass test chamber, which can readily be altered to include a direct see-through path defined by thin entrance and exit windows. The calibration will then be accomplished by the use of low energy monoenergetic electrons, selected by a beta-ray spectrometer, and by the use of the UCLA Van de Graaff. If the tests in the brass chamber show satisfactory operation, the resolution and uniformity of volume response will be carefully examined using the tissue-equivalent chamber and the coincidence set-up in the proton beam to examine various portions of the sensitive volume, since this ultimately is the test which must be successfully passed before meaningful studies of proton energy event distributions may be initiated. It might be mentioned that the results of a great deal of experimental work with similar types of tissue-equivalent proportional counters have been published with no explicit mention of a testing procedure as extensive as that which ultimately revealed defects in the initial electrode design of this program.

Finally, an intensive effort should be made to completely characterize the response to high energy protons of both the 1 mm spherical silicon Au-i-Al detectors and the 1 mm spherical plastic scintillating beads. In addition to being useful for studies of high energy proton energy event distributions occurring in anatomical situations in which the use of proportional counters is impossible due to their inherently large size, they may also be used in other geometries to investigate the minidosimetric distributions at bone-tissue interfaces, etc., and for situations in which it is desired to simulate larger tissue volumes than is practical with proportional counters.

REFERENCES

1. H. H. Rossi and W. Rosenzweig, "A device for the measurement of dose as a function of specific ionization," Radiology 64, 404-411 (1955).

2. H. H. Rossi and W. Rosenzweig, "Measurements of neutron dose as a function of linear energy transfer," Rad. Res. 2, 417-425 (1955).

3. H. H. Rossi, "Specification of radiation quality," Rad. Res. 10, 522-531 (1959).

4. H. H. Rossi, M. H. Biavati, and W. Gross, "Local energy density in irradiated tissues," Rad. Res. 15, 431-439 (1961).

5. H. H. Rossi, "Spatial distribution of energy deposition by ionizing radiation," Rad. Res. 2, Supplement 290-299 (1960).

6. W. H. Barkas and M. J. Berger, "Tables of Energy Losses and Ranges of Heavy Particles," in Studies of Penetration of Charged Particles in Matter, National Academy of Sciences - National Research Council Publication 1133, Washington, D. C., 1964.

7. J. Neufeld and W. S. Snyder, "Estimates of Energy Dissipation by Heavy Charged Particles in Tissue," in Selected Topics in Radiation Dosimetry, International Atomic Energy Agency, Vienna, Austria, 1961.

8. T. Jorgensen, "The Dependence of Stopping Power on Chemical Binding," in Penetration of Charged Particles in Matter, National Academy of Sciences - National Research Council Publication 752, Washington, D. C., 1960.

9. W. H. Bragg, Studies in Radioactivity, (Macmillan and Co., Ltd., London, 1912), p. 94.

10. W. H. Bragg, "The consequences of the corpuscular hypothesis of the γ and x rays and the range of β rays," Phil. Mag. 20, 386-416 (1910).

11. L. H. Gray, The Absorption of Penetrating Radiation," Proc. Roy. Soc., A122, 647-668, London, 1928.

12. L. H. Gray, "An Ionization Method for the Absolute Measurement of γ-ray Energy," Proc. Roy. Soc., A156, 578-596, London, 1936.

13. L. H. Gray, Brit. J. Radiol. 10, 600, 721 (1937).

14. R. Serber, "Nuclear reactions at high energies," Phys. Rev. 72, 1114 (1947).

15. W. E. Kinney and C. D. Zerby, "Calculated Tissue Current-to-Dose Conversion Factors for Nucleons of Energy Below 400 MeV," in Proceedings of the Second Symposium on Protection Against Radiations in Space, NASA SP-71, Gatlinburg, Tennessee, 1964.

16. C. D. Zerby and W. E. Kinney, "Calculated Current-to-Dose Conversion Factors for Nucleons Below 400 MeV," ORNL-TM-1038, 1965.

17. R. Wallace, P. G. Steward, and C. Sondhaus, "Primary- and Secondary-Proton Dose Rates in Spheres and Slabs of Tissue," in Proceedings of the Second Symposium on Protection Against Radiations in Space, NASA SP-71, Gatlinburg, Tennessee, 1964.

18. J. E. Turner, C. D. Zerby, R. L. Woodyard, H. A. Wright, W. E. Kinney, W. S. Snyder, and J. Neufeld, "Calculation of radiation dose from protons to 400 MeV," Health Physics 10, 783-808 (1964).

19. J. Neufeld, W. S. Snyder, J. E. Turner, and H. Wright, "Calculation of radiation dose from protons and neutrons to 400 MeV," Health Physics 12, 227-237 (1966).

20. W. Whaling, "Stopping Power at Low Energies," in Penetration of Charged Particles in Matter, National Academy of Sciences-National Research Council Publication 752, Washington, D. C., 1960.

21. N. Metropolis, R. Bivins, M. Storm, A. Turkevich, J. M. Miller, and G. Friedlander, "Monte Carlo calculations on intranuclear cascades. I. Low-energy studies," Phys. Rev. 110, 185 (1958).

22. N. Metropolis, R. Bivins, M. Storm, J. M. Miller, G. Friedlander, and A. Turkevich, "Monte Carlo calculations on intranuclear cascades. II. High-energy studies and pion processes," Phys. Rev. 110, 204 (1958).

23. H. W. Bertini, "Low energy intranuclear cascade calculation," Phys. Rev. 131, 1801 (1963).

24. H. W. Bertini, "Monte Carlo Calculations for Intranuclear Cascades," in Proc. of Symp. on Protection Against Radiation Hazards in Space, TID-7652, Gatlinburg, Tennessee, 1962.

25. I. Dostrovsky, Z. Fraenkel, and L. Winsberg, "Monte Carlo calculations of nuclear evaporation processes. IV. Spectra of neutrons and charged particles," Phys. Rev. 118, 781 (1960).

26. I. Dostrovsky, P. Rabinowitz, and R. Bivins, "Monte Carlo calculations of nuclear evaporation processes. I. Systematics of nuclear evaporation," Phys. Rev. 111, 1659 (1958).

27. C. J. Bakker and E. Segre, "Stopping power and energy loss for ion pair production for 340 MeV protons," Phys. Rev. 81, 489-492 (1951).

28. H. V. Larson, "Energy loss per ion pair for protons in various gases," Phys. Rev. 112, 1927-1928 (1958).

29. R. A. Lowry and G. H. Miller, "Ionization yield of protons in nitrogen and argon," Phys. Rev. 109, 826-831 (1958).

30. W. D. Allen and A. T. G. Ferguson, Harwell Report AERE NP/R 1720, 1955.

31. J. A. Phipps, J. W. Boring, and R. A. Lowry, "Total ionization in argon by heavy ions of energies 8 to 100 keV," Phys. Rev. 135, A36-A39 (1964).

32. F. R. Shonka, J. E. Rose, and G. Failla, "Conducting Plastic Equivalent to Tissue, Air and Polystyrene," 2nd UN Intern. Conf. on Peaceful Uses of Atomic Energy (Health and Safety, Dosimetry and Standards), Geneva; Proceedings 21, 184 (1958) (P/753USA).

33. R. S. Caswell, "Neutron-insensitive proportional counter for gamma-ray dosimetry," Rev. Sci. Instr. 31, 869 (1960).

34. W. Rosenzweig and H. H. Rossi, "Statistical Fluctuations in the Energy Loss of 5.8 MeV Alpha Particles Passing through an Absorber of Variable Thickness," AEC Report, NYO-10716, 1963.

35. L. Landau, J. Phys. (U.S.S.R.) 8, 201 (1944).

36. K. R. Symon, thesis (Harvard University, 1948).

37. B. Rossi, High-Energy Particles (Prentice-Hall, Inc., Englewood Cliffs, N. J., 1952), pp. 29-37.

38. P. W. Benjamin, C. D. Kemshall, and J. Redfearn, "A High Resolution Spherical Proportional Counter," AWRE Report No. NR 1/64.